Experimental Evaluation of a Structure-Based Connectionist Network for Fault Diagnosis of Helicopter Gearboxes

V. B. Jammu*
Graduate Research Assistant
Mem. ASME

K. Danai
Associate Professor
Mem. ASME

Department of Mechanical Engineering,
University of Massachusetts,
Amherst, MA

D. G. Lewicki
Mem. ASME
Vehicle Technology Center,
U.S. Army Research Laboratory,
NASA Lewis Research Center,
Cleveland, OH

This paper presents the experimental evaluation of the Structure-Based Connectionist Network (SBCN) fault diagnostic system introduced in the preceding article (Jammu et al., 1998). For this, vibration data from two different helicopter gearboxes: OH-58A and S-61, are used. A salient feature of SBCN is its reliance on the knowledge of the gearbox structure and the type of features obtained from processed vibration signals as a substitute to training. To formulate this knowledge, approximate vibration transfer models are developed for the two gearboxes and utilized to derive the connection weights representing the influence of component faults on vibration features. The validity of the structural influences is evaluated by comparing them with those obtained from experimental RMS values. These influences are also evaluated by comparing them with the weights of a connectionist network trained through supervised learning. The results indicate general agreement between the modeled and experimentally obtained influences. The vibration data from the two gearboxes are also used to evaluate the performance of SBCN in fault diagnosis. The diagnostic results indicate that the SBCN is effective in detecting the presence of faults and isolating them within gearbox subsystems based on structural influences, but its performance is not as good in isolating faulty components, mainly due to lack of appropriate vibration features.

1 Introduction

Fault diagnosis of helicopter gearboxes is generally performed by studying the vibration features extracted from accelerometers mounted on the housing. The need to simultaneously consider the numerous vibration features for fault diagnosis has inspired the use of pattern classifying neural networks. However, gearbox fault data is usually not available to train the weights of neural networks. As a remedy, a diagnostic system has been introduced (Jammu et al., 1998) that uses knowledge of gearbox structure and characteristics of the features of vibration to define the influences of faults on features. These structural and featural influences are then incorporated as the connection weights of a Structure-Based Connectionist Network (SBCN). In this system, the vibration features are abnormality-scaled and then propagated through the connection weights of SBCN to obtain fault possibility values for each component in the gearbox.

In this paper, the effectiveness of the proposed diagnostic system is evaluated experimentally using data from two different helicopter gearboxes: OH-58A and S-61. In Section 2, the experimental setup and signal processing for these two gearboxes is discussed. In Section 3, the structural and featural influences are derived, and in Section 4 the validity of the structural influences obtained for the OH-58A gearbox is evaluated by comparing the structural influences with those obtained from experimental root mean square values of vibration as well as the weight values of a neural network of similar structure as SBCN, but trained by supervised learning. Sections 5 and 6 present the fault detection and diagnostic results.

2 Experimental

Measurement-fault data from two different helicopter gearboxes were used to evaluate the performance of the SBCN. The data were obtained from an OH-58A main rotor gearbox (see Fig. 1) and several S-61 gearboxes (see Fig. 2). Unlike the OH-58A, the S-61 helicopter is two-engined, where the engines each drive the left or right input spur gear. The left side input spur gear also drives a thru-shaft which transmits power to an accessory gearbox.

Experimental vibration data for the OH-58A gearbox were collected at the NASA Lewis Research Center as part of a joint NASA/Navy/Army advanced lubricants program (Lewicki et al., 1992). Various component failures in the OH-58A transmission were produced during accelerated fatigue tests. The vibration signals were recorded by eight piezoelectric accelerometers (frequency range of up to 10 KHz) using an FM tape recorder. The signals were recorded once every hour, for about one to two minutes per recording (using a bandwidth of 20 KHz). Two magnetic chip detectors were also used to detect the debris caused by component failures. The location and orientation of the accelerometers are shown in Fig. 3. The OH-58A gearbox was run under a constant load and was disassembled and inspected periodically, or when one of the chip detectors indicated a failure. A total of eleven failures occurred during these tests. They consisted of three cases of planet bearing pitting fatigue, three cases of sun gear pitting fatigue, two cases of top housing cover cracking, and one case each of spiral bevel pinion pitting fatigue, mast bearing micropitting, and planet gear pitting fatigue.

For the S-61 gearbox (see Fig. 2), vibration data were obtained at Sikorsky Aircraft Test Cells for three gearboxes that had been rejected in the field. Vibration signals were measured by ten piezoelectric accelerometers (see Fig. 4) at various operating torque levels, and were recorded by two digital tape recorders with bandwidth capacity of up to 160 kHz. Four snap-

* Presently with GE Corporate Research & Development, Schenectady, New York.

Contributed by the Power Transmission and Gearing Committee for publication in the JOURNAL OF MECHANICAL DESIGN. Manuscript received April 1996. Associate Technical Editor: B. Ravani.

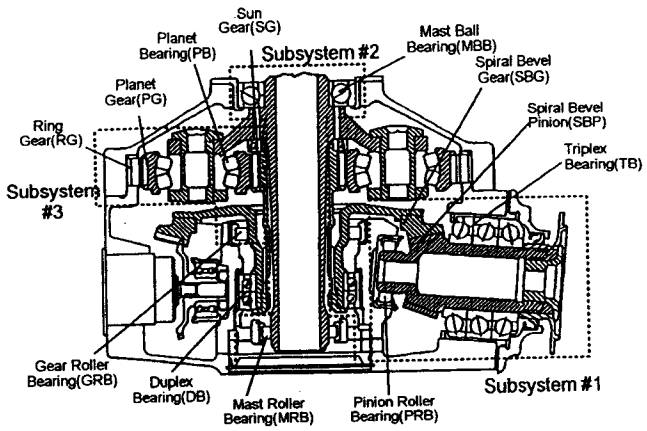

Fig. 1 Layout of the various components in the OH-58A gearbox. The figure also shows division of the gearbox into subsystems for diagnostic purposes.

shots of the vibration signals were recorded for each gearbox within an interval of five minutes. In addition, an inductive debris monitor was used to detect the presence of residues caused by component failures, and a tachometer mounted on the tail take-off shaft to measure the rotational frequency.

The faults associated with the S-61 gearboxes were fewer in number as compared to those in the OH-58A gearbox. The first S-61 gearbox (Serial No. 1089) had produced high vibration levels during field operation. This high vibration is now speculated to be caused by an out-of-balance thru-shaft. Since this particular abnormality is difficult to detect physically, it was undetected by technicians when this gearbox was disassembled and inspected. As a remedy, however, the gearbox was overhauled and the old spiral bevel gear was replaced with a new one. This gearbox is hereafter referred to as No. 1089N (New) and used to represent a normal S-61 gearbox despite the presence of the out-of-balance thru-shaft. This was done due to lack of data from a completely normal S-61 gearbox. Upon inspection, a planet bearing spall was observed in the second S-61 gearbox (No. 1045) and a sun gear failure in the third gearbox (No. 1023).

In order to extract the vibration features, the vibration signals from both gearboxes were digitized and processed by a commercially available signal analyzer (Stewart Hughes Ltd., 1986). Overall, fifty four vibration features were extracted from each accelerometer for the OH-58A gearbox. Out of these features, thirty five features were gear related features (seven for each of the five gears). The remaining nineteen features were indicators of either general faults (e.g., wear and out-of-balance), or general gear and bearing faults. The detailed description of these features is included in (Chin, 1992). For S-61 gearboxes, only statistical analysis and signal averaging could be performed due to unavailability of the signal analyzer. Therefore, the data from the S-61 gearboxes are not as complete as those for the OH-58A gearbox. Nevertheless, they are included in the analysis so as to provide a more comprehensive evaluation of SBCN.

3 Structural and Featural Influences

The structural influences for the OH-58A gearbox were obtained through five primary vibration travel paths: (1) Duplex Bearing-Spiral Bevel mesh-Triplex Bearing, (2) Duplex Bearing-Sun-Planet mesh-Ring Gear (3) Mast Roller Bearing-Main Shaft-Mast Ball Bearing (4) Ring Gear-Planet Bearing-Mast Ball Bearing, and (5) Duplex Bearing-Sun Planet mesh-Mast Ball Bearing. The first travel path was in connection to Accelerometers 4, 5, and 6, whereas all the other paths were connected to Accelerometer 1, 2, 3, 6, 7, and 8. The RMS values of vibration were then computed using the lumped-mass model of these paths with excitation sources at each of the gearbox components. These RMS values were then used as the basis for defining the fuzzy structural influences between each component-accelerometer pair (see Table 1).

The structural influences in Table 1 indicate that all of the components in the gearbox are covered by the accelerometers, and that some accelerometers have identical influences with respect to the components. Although these influences are not completely accurate, due to their neglect of the orientation of accelerometers and other approximations (Jammu et al., 1998), they can still be used for an overall assessment of the effectiveness of various accelerometers and their redundancy. For example, the influences in Table 1 are identical for Accelerometers 1, 2, 3, 6, 7, and 8. This would indicate that one or more of these accelerometers can be discarded without any drastic effect on fault diagnostic effectiveness. However, it should be noted that the strategy used in SBCN relies on the averaging effect of accelerometers and that it will not function without a certain level of overlap in accelerometer coverage.

The structural influences for the S-61 gearbox needed to be defined in a more approximate manner, since the information about the location and type of bearings was unavailable due to proprietary reasons. For the S-61 gearbox, nine primary vibration travel paths were identified, and structural influences of components were defined as functions of the distance between each component and accelerometer. The analogy for using dis-

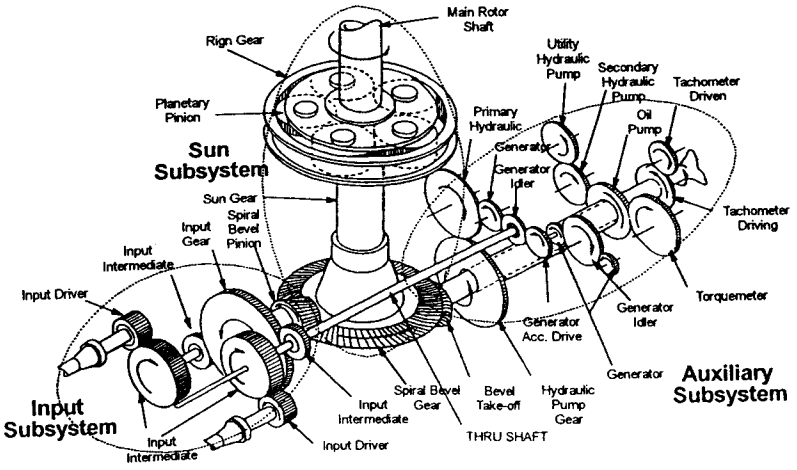

Fig. 2 Layout of the various components in the S-61 gearbox. The figure also shows division of the gearbox into subsystems for diagnostic purposes.

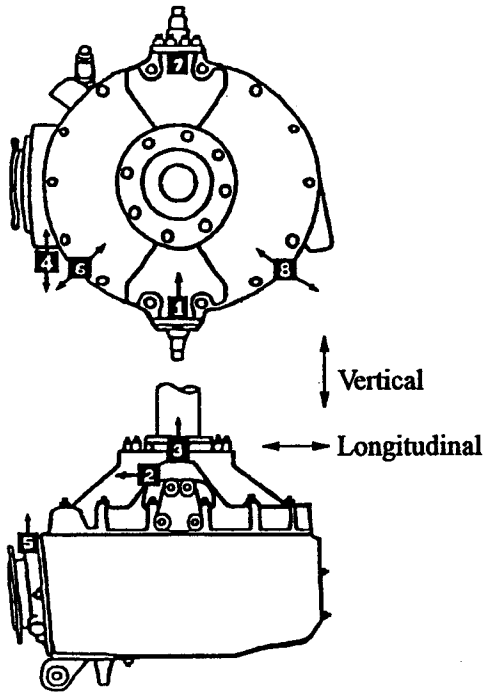

Fig. 3 Location and orientation of the accelerometers on the OH-58A test stand

tance here is that longer travel paths result in stronger vibration attenuation, so they are expected to have smaller influences. Using this principle, the influences of the S-61 gearbox components on the ten accelerometers were obtained, which due to space limitations are not included here. Interested readers may refer to (Jammu, 1996).

The featural influences were defined for individual vibration features according to the type of fault they are supposed to represent. For example, bearing related features such as Envelope Band and Tone Energy are assigned High in association with gearbox bearings. Similarly, the signal averaged features for the five gears in the OH-58A gearbox are assigned High with respect to these gears. Features which are indicators of faults in all rotating elements in the gearbox are assigned an influence of Medium for gears as well as bearings.

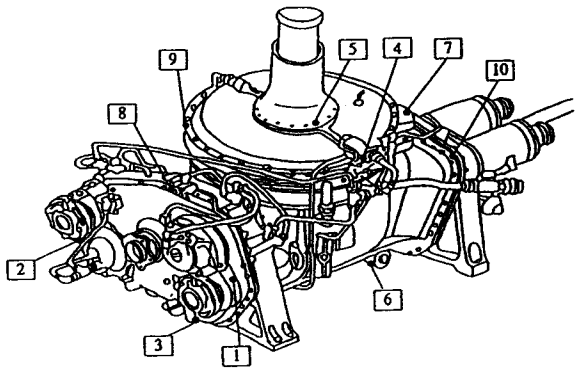

Fig. 4 Location of accelerometers on the S-61 test stand

Table 1 Structural influences between the components of the OH-58A gearbox and the eight accelerometers.

Comp/Acc	1	2	3	4	5	6	7	8
Triplex Bearing	-	-	-	H	H	-	-	-
Spiral Bevel Pinion	-	-	-	H	H	-	-	-
Pinion Roller Bearing	-	-	-	H	H	-	-	-
Spiral Bevel Gear	-	-	-	H	H	-	-	-
Duplex Bearing	M	M	M	H	H	M	M	M
Gear Roller Bearing	M	M	M	H	H	M	M	M
Mast Roller Bearing	M	M	M	-	-	M	M	M
Main Shaft	M	M	M	-	-	M	M	M
Mast Ball Bearing	M	M	M	-	-	M	M	M
Sun Gear	H	H	H	L	M	H	H	H
Planet Bearing	H	H	H	L	M	H	H	H
Planet Gear	H	H	H	L	M	H	H	H
Ring Gear	H	H	H	L	M	H	H	H

The structural and featural influences constitute the basis of the SBCN connection weights. As discussed in Jammu et al. (1998) diagnosis in SBCN is performed hierarchically, first isolating the faulty subsystems, and then faulty components. As such, only the average of the structural influences associated with each subsystem is used as the connection weight v_{ik} of SBCN to yield the fault possibility values $p_k(t)$ associated with each subsystem, according to (Jammu et al., 1997):

$$p_k(t) = \sum_{i=1}^{n} f_i(t) v_{ik} \tag{1}$$

In subsystem diagnosis, $f_i(t)$ denotes the average abnormality-scaled value of general features. In the second stage of fault diagnosis, at the component level, the combination of structural and featural influences are used as v_{ik}, and $f_i(t)$ consist of individual abnormality-scaled features.

4 Evaluation of Influences

As explained in Jammu et al. (1998) the structural influences representing the proximity effect of component faults on accelerometer readings were obtained from the RMS value of the frequency response of the lumped-mass model of the gearbox. In this case, however, the actual RMS values of the vibration were available at several fault instances for the OH-58A gearbox, which could also be used to yield a set of experimentally obtained structural influences. In order to evaluate the modeled influences, a comparison between these two sets of structural influences was conducted. The experimental influences were obtained by normalizing the experimental RMS values when a faulty component had been detected and using them as the basis for assigning the level of fuzzy influences (see Table 2). The results in Table 2 indicate mixed agreement between experimental and structural influences. For example, the structural influences of Sun Gear, Planet Bearing, and Planet Gear on Accelerometers 1, 2, and 3 are close to the experimentally obtained influences, but the influence of Mast Ball Bearing on Accelerometers 2 and 3 do not match. In this case, mismatch between the two sets of influences may be due to: (1) the limitation of the RMS value in reflecting the change in vibration as a result of various component faults (e.g., Mast Ball Bearing micropitting), (2) variation in the level of change of the RMS values as a function of the type and size of the fault, and/or (3) lack of faults in every component of the OH-58A gearbox, which limits the basis for determining the influences for every gearbox component. A similar comparison of influences could not be performed for the S-61 gearbox due to unavailability of an adequate number of faults in that data.

Defining influences based on an approximate model of the gearbox was motivated by the need to avoid supervised training of SBCN. However, given that experimental data were available for the OH-58A gearbox, an evaluation of the structural influences could be performed by comparing them with the weights of a connectionist network structurally similar to SBCN, but

Table 2 Influences between accelerometers and gearbox components obtained form experimental RMS values of vibration for the OH-58A gearbox. For comparison, the influences from the lumped-mass model are shown inside parentheses.

Influences from RMS Values of Vibration										
Acc. /Parts	Spiral Bevel Pinion		Mast Ball Bearing		Sun Gear		Planet Bearing		Planet Gear	
1	-	(-)	-	(-)	H	(H)	M	(H)	M	(H)
2	M	(-)	-	(H)	M	(H)	M	(H)	M	(M)
3	M	(-)	-	(H)	M	(H)	H	(H)	M	(M)
4	L	(H)	-	(-)	H	(L)	-	(-)	M	(-)
5	H	(H)	-	(-)	H	(M)	H	(M)	-	(M)
6	L	(-)	-	(-)	L	(H)	M	(H)	L	(H)
7	-	(-)	-	(-)	H	(H)	M	(H)	L	(H)
8	-	(-)	-	(-)	M	(H)	M	(H)	M	(H)

trained by supervised learning. For this purpose, the OH-58A gearbox was divided into three subsystems (see Fig. 1), and the supervised network having three output units for the three subsystems and eight input units for the eight accelerometers was trained using least mean square (LMS) learning. The weights of this network were trained until the number of false alarms and misdiagnoses were reduced to zero. The trained weights were then normalized and converted into fuzzy variables for comparison with the structural influences obtained from the lumped-mass model of the gearbox. Table 3 includes the influences of the two networks, where the modeled influences (inside parentheses) represent the averages of component influences within each subsystem (see Table 1). The results in Table 1 indicate general agreement between the trained weights and modeled influences. Some of the trained weights had negative values (indicated by '*') which is inevitable due to the use of LMS learning. However, all of these negative weights were quite small in magnitude, which makes them consistent with their modeled Nil counterparts (denoted by '-'). As in the case of influences from the RMS values (Table 2), some of the mismatches in Table 3 are expected to be due to the limited number of faults represented in the experimental data. For example, the considerably different influence of Subsystem 2 on Accelerometer 1, or Subsystem 3 on Accelerometer 1, is attributed to the lack of specific faults in these subsystems that would lead to a more accurate influence on Accelerometer 1.

The comparison between the modeled structural influences and those obtained from the supervised neural network indicates that the modeled influences are in good agreement with the trained influences, and that the lumped-mass modeling used here provides an acceptable set of structural influences for SBCN.

5 Fault Detection Results

The Fault Detection Network (FDN) in the proposed diagnostic system (Fig. 1 in Jammu et al., 1998) is used first to identify the presence of faults in the gearbox. Fault diagnosis is then performed when the presence of a fault is prompted. In this section, the fault detection results obtained for the OH-58A and S-61 gearboxes are presented.

Table 3 Normalized weight values of the supervised connectionist network. For comparison, the subsystem influences of SBCN are included inside parentheses. A '*' indicates a negative weight value.

Acc.	Subsystem 1		2		3	
1	*	(-)	*	(M)	*	(H)
2	*	(-)	H	(M)	H	(H)
3	*	(-)	*	(M)	L	(H)
4	H	(H)	*	(-)	*	(L)
5	M	(H)	*	(-)	H	(M)
6	M	(M)	*	(M)	H	(H)
7	M	(-)	L	(M)	H	(H)
8	*	(-)	H	(M)	M	(H)

5.1 OH-58A Detection Results.

A total of eight FDNs, one for each of the eight OH-58A accelerometers, were used. The inputs to each FDN were the nineteen general features not specific to any particular gear or bearing. The initial weight values of the FDNs were set as the values of the first set of features for each of the five tests, and were subsequently adapted using 50 adaptation sweeps for each training batch. The occurrence of a fault was prompted when any of the FDNs indicated a fault. The detection results for individual test sets obtained from the FDNs are shown in Table 4. A '-' in this table indicates normal conditions, whereas a '1' indicates the presence of a fault. The expected detection results are indicated inside parentheses. The results for Test 1 indicate that the presence of faults were detected on Days 5, 7, and 8, while faults were expected to be present from Days 5 through 9. Of course, it should be noted that the gearbox was not inspected on a daily basis, so the actual condition of the gearbox is unknown for each day of the tests. In Test 1, which was run for 9 days, a fault was actually observed only on Day 9 during routine inspection of the gearbox (indicated by 1*). However, based on an inspection of the vibration features, it was estimated that the fault could have been present as early as Day 5. For the other tests, the days when the faults were actually observed are also indicated by 1*. While it is discouraging to note that Day 6 of Test 1 was classified as normal although a fault was present on Day 5, the results are in agreement with observations by experts who believe that sometimes increased noise levels immediately after the occurrence of faults mask the effect of faults on vibration features. For the other tests, the results indicate that except for an undetected fault in Test 3 and a false alarm in Test 4, excellent fault detection was obtained. It should also be noted that the fault on Day 9 of Test 3 was a hairline crack, that is perhaps undetectable through vibration monitoring. The quality of fault detection in the proposed system is particularly important to the overall diagnostic results, since it is only after a fault is detected that SBCN is engaged in diagnosis.

Table 4 Fault detection results for the OH-58A gearbox. A '-' indicates normality and a '1' represents the presence of a fault. For reference, the expected faults determined by an expert are included inside the parentheses, with '*' indicating actual observation of the fault.

Day	FDN: Predicted and Actual Failures									
	Test 1		Test 2		Test 3		Test 4		Test 5	
1	-	(-)	-	(-)	-	(-)	-	(-)	-	(-)
2	-	(-)	-	(-)	-	(-)	-	(-)	-	(-)
3	-	(-)	-	(-)	1	(1)	-	(-)	-	(-)
4	-	(-)	-	(-)	1	(1*)	-	(-)	-	(-)
5	1	(1)	-	(-)	-	(-)	-	(-)	-	(-)
6	-	(1)	-	(-)	-	(-)	-	(-)	-	(-)
7	1	(1)	-	(-)	-	(-)	-	(-)	-	(-)
8	1	(1)	-	(-)	-	(-)	-	(-)	-	(1)
9	-	(1*)	-	(-)	-	(1*)	-	(-)	1	(1)
10					-	(-)	1	(1)	-	(1)
11					1	(1)	1	(1)	-	(1*)
12					1	(1)	1	(1*)		
13					-	(1*)	1	(-)		
14							1	(1)		
15							1	(1*)		

5.2 **S-61 Detection Results.** As noted earlier, in the absence of normal data for the S-61 gearboxes, vibration data from S-61 Gearbox No. 1089N were used to represent normal behavior of this gearbox. The ten statistical features from the three S-61 gearboxes were arranged into a single set of data with a total of 16 snapshots. The first set of four snapshots was from Gearbox No. 1089N to represent the normal behavior of the S-61 gearboxes, and the subsequent sets of twelve snapshots were from Gearboxes No. 1089, No. 1045, and No. 1023. Ten data sets, one from each of the ten accelerometers, were then used sequentially as inputs to the ten FDNs for fault detection. The fault detection results obtained for the three S-61 gearboxes are included in Table 5. As before, a '1' in this table indicates identification of a fault. The results indicate that the first four snapshots from Gearbox No. 1089N were identified as normal and that the presence of all of the faults in Gearboxes No. 1089, No. 1045 and No. 1023 were correctly identified.

In summary, the detection results obtained for the two gearboxes (Tables 4 and 5) indicate that the occurrence of most of the faults were identified. This provides assurance that the later stage of diagnostics would not be seriously hampered by the detection phase.

6 Fault Diagnostic Results

In the proposed system, fault diagnosis is performed by the SBCN only after the presence of a fault is detected. In this system, fault diagnosis is performed in two hierarchies, so as to take full advantage of the separation of the structural and featural influences. In the first hierarchy, the gearbox is divided into subsystems (see Figs. 1 and 2) and the faults in individual subsystems are isolated by SBCN based on the structural influences alone. For each subsystem, the weights of SBCN are set equal to the average of the structural influences of the components within that subsystem (see Tables 3 and 7). The inputs to SBCN for this stage of diagnosis consist of the averaged values of abnormality-scaled features from each accelerometer, and its outputs are the fault possibility values for each subsystem. In the second hierarchy, the faulty components within each subsystem are isolated. The inputs to SBCN for this stage of diagnosis are the abnormality-scaled vibration features, and the weights are the product of featural influences and structural influences of the subsystem containing each component. Averaging of fuzzy influences here was obtained by taking the average of upper bounds and lower bounds of individual influences separately, and then defining the fuzzy variable that would match the range. The product of fuzzy influences was obtained by multiplying the upper bounds and lower bounds of fuzzy variables separately and then defining the fuzzy variable for the resultant range.

Table 5 Fault detection results for the S-61 Gearboxes (No. 1089, No. 1045, and No. 1023). A value of '1' indicates identification of a fault, while a '-' indicates normal reading.

Fault detection results for S-61 gearboxes		
Snapshot	Predicted	Actual
1 (1089N)	-	(-)
2 (1089N)	-	(-)
3 (1089N)	-	(-)
4 (1089N)	-	(-)
5 (1089)	1	(1)
6 (1089)	1	(1)
7 (1089)	1	(1)
8 (1089)	1	(1)
9 (1045)	1	(1*)
10 (1045)	1	(1*)
11 (1045)	1	(1*)
12 (1045)	1	(1*)
13 (1023)	1	(1*)
14 (1023)	1	(1*)
15 (1023)	1	(1*)
16 (1023)	1	(1*)

Table 6 Faulty subsystem isolation results for the OH-58A gearbox. The three subsystems in the table are the Input Subsystem (1), the Output Subsystem (2), and the Transmission Subsystem (3). For comparison the actual faults are included inside parentheses with '*' indicating the observed faults.

Faulty Subsystems Isolation for OH-58A									
Day	Test 1		Test 2	Test 3		Test 4		Test 5	
1	-	(-)	- (-)	-	(-)	-	(-)	-	(-)
2	-	(-)	- (-)	-	(-)	-	(-)	-	(-)
3	-	(-)	- (-)	1, 3	(3)	-	(-)	-	(-)
4	-	(-)	- (-)	1, 3	(3*)	-	(-)	-	(-)
5	1, 3	(1, 3)	- (-)	-	(-)	-	(-)	-	(-)
6	-	(1, 3)	- (-)	-	(-)	-	(-)	-	(-)
7	1, 3	(1, 3)	- (-)	-	(-)	-	(-)	-	(-)
8	1, 3	(1, 3)	- (-)	-	(-)	-	(-)	-	(3)
9	-	(1*, 3*)	- (-)	-	(3)	-	(-)	1, 3	(3)
10				-	(-)	3	(3)	-	(3)
11				2, 3	(2, 3)	3	(3)	-	(3*)
12				2, 3	(2, 3)	3	(3*)		
13				-	(2*, 3*)	3	(-)		
14						3	(3)		
15						3	(3*)		

6.1 Faulty Subsystem Isolation. The fault possibility values for the three subsystems of the OH-58A gearbox are shown in Table 6. The results in this table represent the hard-limited fault possibility values (threshold of 0.5) and include, for comparison, the actual condition of the gearbox reported from routine inspection inside parentheses. As before, a '*' indicates actual observation of the fault during inspection of the gearbox. The results in Table 6 indicate that in Test 1, faults in Subsystems 1 and 3 were correctly identified on Days 5, 7, and 8. In Test 3, the faults in Subsystem 3 on Days 3 and 4 were correctly identified, along with a possible fault in Subsystem 1. The housing crack on Day 9 of this test was left unidentified because it was never prompted during the detection phase. Nevertheless, this particular fault (housing crack) could not be isolated by the current SBCN due to absence of features that reflect this fault. Also for this test, faults in Subsystems 2 and 3 were correctly identified on Days 11 and 12. In Test 4, the fault in Subsystem 3 was correctly diagnosed on Days 10, 11, 12, 14 and 15. Moreover, on Day 13 of Test 4, even though the gearbox was supposed to be normal, the SBCN indicated faults in Subsystem 3. This was due to the replacement of the three-planet assembly with a four-planet assembly, which changed the vibration characteristic of Subsystem 3. In Test 5, the fault in Subsystem 3 was correctly identified on Day 9. There was also a misdiagnosis in Subsystem 1.

In summary, the diagnostic results from the gearbox subsystems indicate that all of the 8 subsystem faults were correctly identified in the OH-58A gearbox and that 4 faults were misdiagnosed. Considering that these results were obtained by using structural influences alone as the connection weights of SBCN, the results validate the utility of these influences and of lumped-mass modeling as a means of representing the vibration travel path of gearboxes for their model-based fault diagnosis.

The components of the S-61 gearbox were also divided into three subsystems (see Fig. 2) and the SBCN was first used to isolate faults in these subsystems. The fuzzy influence weights of SBCN for this phase were obtained by averaging the structural influences of the components within each subsystem, as shown in Table 7.

The diagnostic results obtained for the subsystems of S-61 gearboxes are shown in Table 8. As before, the results in this table represent hard-limited fault possibility values (threshold of 0.5) for the three subsystems. The results from the first set of four snapshots of Gearbox No. 1089N indicate that all of the three subsystems are normal. For the next set of four snapshots from Gearbox No. 1089, faults are detected in Subsystems 1

Table 7 Influences of the three S-61 subsystems on the ten accelerometers. The influences are represented as '-' for Nil, 'L' for Low, 'M' for Medium and 'H' for High.

Subsystem/Acc.	1	2	3	4	5	6	7	8	9	10
1	H	H	H	-	-	-	-	H	-	-
2	-	-	-	H	H	H	H	M	H	-
3	L	-	-	-	-	H	-	L	-	H

and 2. Subsystem 1 is suspected as faulty due to the out-of-balance in the Thru-Shaft. Note that this Subsystem would have been identified as normal if the first four snapshots from Gearbox No. 1089N did not have the problem of Thru-Shaft out-of-balance. Subsystem 2 is tagged as faulty because of the replaced spiral bevel gear. For snapshots 9 through 12 from Gearbox No. 1045, Subsystems 1 and 2 were identified as faulty. Subsystem 2 was tagged as definitely faulty (possibility value of 1) because of the planet bearing spall, and Subsystem 1 was tagged because of the Thru-Shaft problem related to Gearbox No. 1089N. For Gearbox No. 1023 (snapshots 12 through 16) a fault in Subsystem 2 was indicated. In this case, the fault was a sun gear failure which the SBCN correctly diagnosed.

Faulty subsystem isolation results from the S-61 gearboxes indicate that all of the 3 faults in the subsystems were identified, and that faults were misdiagnosed in Subsystem 2 for Gearbox No. 1089 and in Subsystem 1 for Gearbox No. 1045. In view of the incomplete information pertaining to (1) unavailability of normal data for the three S-61 gearboxes, (2) unavailability of the type and location of bearings in the gearboxes, and (3) lack of gear and bearing specific features, the results obtained from SBCN are remarkably good.

6.2 Faulty Component Isolation. Fault possibility values associated with the components of the OH-58A gearbox obtained from the SBCN are included in Table 9. The results indicate that the diagnostics associated with individual components are not as accurate as those obtained for the subsystems. Briefly, for Test 1, the Spiral Bevel Pinion (SBP) fault in Subsystem 1 and Sun Gear (SG) fault in Subsystem 3 were correctly identified only on Days 5 and 8, respectively, while other components were assigned higher fault possibility values on other days. For Test 3, the three bearing faults in Subsystems 2 and 3 (BRG2 and BRG3, respectively) were correctly identified on Days 3, 4, and 12, but other components were also given high fault possibility values. In Test 4, the bearing fault in Subsystem 3 (BRG3) was correctly identified only on Day 10, while the Sun Gear (SG) fault remained misdiagnosed. In Test 5 the Sun Gear (SG) fault was correctly identified on Day 9, while the Planet Gear (PG) fault was misdiagnosed.

In view of the promising results obtained at the subsystem level which confirm the validity of the structural influences, the cause of diagnostic inaccuracies at the component level should be attributed mainly to the deficiency of gear and bearing specific features used in this study. This is manifested in the strong cross-coupling between these features, illustrated by the maximum values of the correlation coefficient between the gear and bearing features and gear and bearing faults in Table 10. The results indicate reasonable correlation values of 0.49 between the gear features and gear faults, and 0.44 between the bearing features and bearing faults. These numbers, however, are not as impressive when they are compared with the cross-correlation values of 0.57 between gear features and bearing faults, and 0.38 between bearing features and gear faults. The high cross-correlation values in Table 10 indicate that the gear and bearing features do not provide the resolution necessary for faulty component isolation. Another way of noting the strong coupling between the gear and bearing features is illustrated in Fig. 5 where the average values of the gear features ACH and FM4A and bearing features BE and ET from the eight OH-58A accelerometers are plotted for Tests 1 and 3. The results in this figure indicate that as well as the gear feature ACH, the bearing feature BE is affected by the gear faults in the Spiral Bevel Pinion (SBP) and the Sun Gear (SG) on Days 5 and 7 in Test 1, and that both the bearing feature ET and gear feature FM4A reacted to a Planet Bearing Spall on Day 3 of Test 3. The manifestation of the resolution problem caused by the coupling between gear and bearing features is observed in the similar fault possibility values of 0.9 and 0.89 on Day 5 of Test 1 in Table 9 for the

Table 8 Fault subsystem isolation results for S-61 Gearboxes No. 1089N, No. 1089, No. 1045 and No. 1023. The three subsystems in the table are: 1 for input, 2 for sun, and 3 for auxiliary. For comparison the actual faults are included inside parentheses with '*' indicating the observed faults.

Faulty Subsystem Isolation for S-61		
Snapshot	Predicted	Actual
1 (1089N)	-	(-)
2 (1089N)	-	(-)
3 (1089N)	-	(-)
4 (1089N)	-	(-)
5 (1089)	1, 2	(1)
6 (1089)	1, 2	(1)
7 (1089)	1, 2	(1)
8 (1089)	2	(1)
9 (1045)	1, 2	(2*)
10 (1045)	1, 2	(2*)
11 (1045)	2	(2*)
12 (1045)	2	(2*)
13 (1023)	2	(2*)
14 (1023)	2	(2*)
15 (1023)	2	(2*)
16 (1023)	2	(2*)

Table 9 Faulty component isolation by SBCN for the OH-58A gearbox. The components listed are -SBP: Spiral Bevel Pinion; SBG: Spiral Bevel Gear; BRG1: Bearings in Subsystem (SS); 1, BRG2: Bearings in Subsystem 2; SG: Sun Gear; PG: Panet Gear; and BRG3: Bearings in Subsystem 3. As before, '*' indicates observation of the faulty component.

Faulty Component Isolation for OH-58A								
	SS 1			SS 2	SS 3			
Days	SBP	SBG	BRG1	BRG2	SG	PG	RG	BRG3
Test 1								
1 to 4	-	-	-	-	-	-	-	-
5	0.90*	0.62	0.89	-	0.52*	0.73	0.12	0.86
6	-*	-	-	-	-*	-	-	-
7	0.68*	0.43	0.79	-	0.67*	1.00	0.23	0.72
8	0.65*	0.74	0.18	-	0.98*	0.70	0.70	0.33
9	-	-	-	-	-	-	-	-
Test 2								
1 to 9	-	-	-	-	-	-	-	-
Test 3								
1 to 2	-	-	-	-	-	-	-	-
3	0.43	0.77	0.80	-	0.65	0.56	0.71	0.72*
4	0.38	0.60	0.78	-	0.56	0.47	0.04	0.79*
5 to 10	-	-	-	-	-	-	-	-
11	-	-	-	-	0.67	0.79	0.52	-*
12	-	-	-	0.74*	0.67	0.71	0.55	1.00*
13	-	-	-	-*	-	-	-	-*
Test 4								
1 to 9	-	-	-	-	-	-	-	-
10	-	-	-	-	0.34	0.41	0.75	0.79*
11	-	-	-	-	0.54	0.53	0.79	-*
12	-	-	-	-	0.59	0.50	0.91	0.64*
13	-	-	-	-	0.72	0.85	0.83	1.00
14	-	-	-	-	0.81*	0.90	0.88	0.68
15	-	-	-	-	0.79*	0.90	0.93	0.48
Test 5								
1 to 8	-	-	-	-	-	-	-	-
9	0.58	0.24	0.68	-	0.60*	0.54*	0.50	0.58
10 to 11	-	-	-	-	-*	-*	-	-

Table 10 Maximum values of correlation coefficients between features and faults. The values inside parentheses are the expected ideal values.

Fault-feature correlation coefficients		
Features/Faults	Gear Faults	Bearing Faults
Gear Features	0.49 (1)	0.57 (0)
Bearing Features	0.38 (0)	0.44 (1)

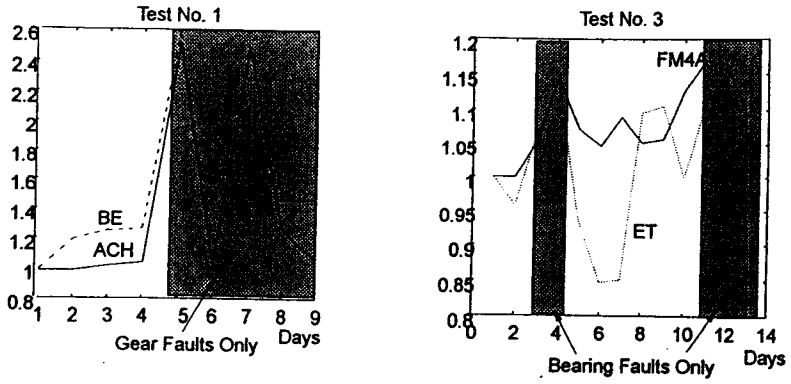

Fig. 5 The average values of gear features (ACH and FM4A) and bearing features (BE and ET) from the eight OH-58A accelerometers for Tests 1 and 3. The results illustrate that both ACH and BE are affected by gear faults in Test 1, and both FM4A and ET are affected by bearing faults in Test 3. The grey area denotes the period when faults were present.

Spiral Bevel Pinion (SBP) and bearings in Subsystem 1 (BRG1). Based on the results in Table 9 one can conclude that the unsupervised pattern classification scheme incorporated in this research cannot be a substitute for well defined features, and that a more effective set of features with smaller cross-correlation values is needed for diagnosis at the component level.

7 Conclusion

The effectiveness of the Structure-Based Connections Network (SBCN) was experimentally evaluated in diagnosis of OH-58A and S-61 helicopter gearbox faults. Approximate vibration transfer models were developed for these gearboxes and were used to define structural influences to relate component faults to accelerometer readings. The structural influences were evaluated by comparing them with influences obtained from the RMS values of vibration and weights of a supervised connectionist network. The results indicate that the approximate vibration transfer model used can capture the overall relation between the component faults and vibration signals. The Fault Detection Network (FDN) was then applied to identify the presence of faults in the OH-58A and S-61 gearboxes. The results from the fault detection phase indicate that the presence of the majority of faults were detected without any false alarms. In order to perform fault diagnosis, the vibration features were scaled for abnormality and fed to the SBCN. Promising diagnostic results were obtained from SBCN for both gearboxes at the subsystem level, whereas results at the component level lacked resolution due to the strong cross-correlation among features. While the diagnostic results at the component level are not accurate enough to qualify SBCN for practical application, the results at the subsystem level validate the premise that knowledge of the gearbox structure can be used as the basis for model-based fault diagnosis of gearboxes. Such an approach, when integrated with more effective features, will undoubtedly lead to a fault diagnostic system suited for practical application.

References

Chin, H., 1992, *Vibration Analysis of an OH-58A Main Rotor Transmission, Technical Report,* Department of Mechanical Engineering, University of Massachusetts, Amherst, MA 01003.

Lewicki, D. G., Decker, H. J., and Shimski, J. T., 1992, *Full-Scale Transmission Testing to Evaluate Advanced Lubricants,* NASA TM-105668, AVSCOM TR-91-C-035.

Jammu, V. B., 1996, "Structure-Based Connectionist Network for Fault Diagnosis of Helicopter Gearboxes," PhD thesis, University of Massachusetts, Amherst, MA 01003.

Jammu, V. B., Danai, K., and Lewicki, D. G., 1998, "Structure-Based Connectionist Network for Fault Diagnosis of Helicopter Gearboxes," ASME JOURNAL OF MECHANICAL DESIGN, Vol. 120, No. 1, pp. 100–105.

Stewart Hughes Limited, 1986, *MSDA* User's Guide, Technical Report, Southampton, UK.